Zoosyst. Evol. 94 (2) 2018, 325–337 | DOI 10.3897/zse.94.22685

PENSOFT

für Natur MUSEUM FÜR NATURKUNDE BERLIN

Three new species of the '*Geophagus*' *brasiliensis* species group from the northeast Brazil (Cichlidae, Geophagini)

José L. O. Mattos[1], Wilson J. E. M. Costa[1]

1 *Laboratory of Systematics and Evolution of Teleost Fishes, Institute of Biology, Federal University of Rio de Janeiro, Rio de Janeiro, Caixa Postal 68049, CEP 21944-970, Rio de Janeiro, Brazil*

http://zoobank.org/E446D128-9ACA-4CFB-944F-B15492ABFDC2

Corresponding author: *José L. O. Mattos* (jlomattos@gmail.com); *Wilson J. E. M. Costa* (wcosta@acd.ufrj.br)

Received 1 December 2017
Accepted 21 June 2018
Published 6 July 2018

Academic editor:
Johannes Penner

Key Words

Atlantic Forest
Biodiversity hotspot
Molecular phylogeny
Neotropical
Systematics
Integrative taxonomy

Abstract

Morphological characters and phylogenetic trees generated by analyses of segments of two mitochondrial genes cytochrome b and cytochrome c oxidase I support recognition of three new species of the '*Geophagus*' *brasiliensis* species group from coastal basins of northeast Brazil. All new species were diagnosed by exclusive morphological characters and exclusive nucleotide transformations. *Geophagus rufomarginatus* sp. n., from the Rio Buranhém Basin, is distinguished from all other species of the group by dorsal-fin lappets with red edges, the presence of longitudinal series of small light blue spots between the anal-fin spines and rays, and non-denticulated gill-rakers; it is closely related to *G. brasiliensis* and *G. iporangensis*. *Geophagus multiocellus* sp. n., from the Rio de Contas Basin, is distinguished from all other species of the group by having small pale blue spots with minute bright blue dots at their centres, that are often vertically coalesced to form short bars on the caudal fin. *Geophagus santosi* sp. n., from the Rio Mariana Basin, is distinguished from all other species of the group by having blue stripes parallel to the dorsal and anal fin rays on their longest portions. *Geophagus multiocellus* and *G. santosi* belong to the same clade of *G. itapicuruensis*. The clade composed by the Rio Paraguaçu Basin species was recovered as the sister group of the other species of the '*G.*' *brasiliensis* species group.

Introduction

The Atlantic Forest is a biodiversity hotspot biome which has suffered degradation and drastic reduction throughout the history of human occupation and development of economic activities (Myers et al. 2000). Consequently, many components of its endemic biodiversity are currently under threat of extinction. This South American natural province (Morrone 2006) shows a high rate of endemism in its remaining fragments (Myers et al. 2000), harboring some endemic species of freshwater fishes, including cichlids (Kullander 2003, Lucena and Kullander 2006, Ottoni 2013, Ottoni and Costa 2008).

The cichlid tribe Geophagini is broadly distributed in South America and presents the greatest diversity among tribes of Neotropical cichlids, comprising 15 genera (López-Fernández et al. 2010). Included species occupy a wide range of ecological niches and exhibit remarkable morphological and behavioural adaptations (López-Fernández et al. 2013, Arbour and López-Fernández 2014). The type genus *Geophagus* Haeckel, 1940 has been diagnosed by the morphology of vertebrae, comprising the presence of epipleural ribs on caudal vertebrae, which are associated with expansions of the swim bladder, and caudal vertebrae more numerous than abdominal (Kullander 1986). However, these morphological features are not shared by all species of the genus. Presently, the genus has been divided into three species groups (Kullander 1998; López-Fernández and Taphorn 2004). Species that fit Kullander's (1986) generic diagnosis were assembled into the *Geophagus sensu stricto* species group, which includes the type species of the genus *Geophagus altifrons* Haeckel, 1840 and other species distributed in northern South America, including the Amazonas, Orino-

co and Parnaíba river basins. Nevertheless, two species groups do not have those morphological characteristics: the '*Geophagus*' *steindachneri* species group, with a trans-Andean distribution between southern Panama and Maracaibo lake region in Venezuela, and the '*Geophagus*' *brasiliensis* species group, geographically widespread in eastern South America, mostly in the Atlantic Forest (Kullander 2003, Mattos et al. 2015). Recent phylogenetic studies (López-Fernández et al. 2010, Ilves et al. 2017) indicate that these three species groups together do not form a monophyletic lineage, and consequently, authors when describing new species of the last two groups have tentatively assigned them to '*Geophagus*', thus using the genus name between apostrophes to designate their uncertain position (Kullander 1998, López-Fernández et al. 2010, Ilves et al. 2017).

Currently, the '*G.*' *brasiliensis* species group comprises five valid species (Kullander 2003; Mattos et al. 2015): *G. iporangensis* Haseman, 1911, from the Rio Ribeira do Iguape Basin; *G. itapicuruensis* Haseman, 1911, from the Rio Itapicuru Basin; *G. obscurus* (Castelnau, 1855), from the coastal section of the Rio Paraguaçu Basin (Lucena and Kullander 2006); *G. diamantinensis* Mattos, Costa & Santos, 2015 from the upper section of the Rio Paraguaçu Basin; and '*G.*' *brasiliensis*, occurring in a broad area along the coastal basins between Bahia state, northeast Brazil, and the La Plata province, northeast Argentina (Kullander 2003, Mattos et al. 2015). The distribution of this species group covers a broad area of the Atlantic Forest and a small area of the Caatinga, a semiarid northeast Brazilian biome (Mattos et al. 2015). This study is the first analysis in which all valid species of the '*G.*' *brasiliensis* species group were sampled and analysed in a molecular phylogenetic framework, besides including populations of three unidentified species from the Atlantic Forest of northeast Brazil exhibiting unique morphological features, which are herein recognised and described as new.

Material and methods

Material

Measurements and counts follow Kullander (1986, 1990) and Kullander & Nijssen (1989). Measurements are presented as percentages of standard length (SL), except subunits of head, which are presented as percentages of head length (HL). Osteological preparations (C&S) were made according to Taylor and Van Dyke (1985). Osteological nomenclature follows Costa (2006). Material examined is deposited in the following ichthyological collections: Ichthyology collection of the Center for Agrarian and Environmental Sciences, Chapadinha (CICCAA); Museu Nacional, Rio de Janeiro (MNRJ); Institute of Biology, Federal University of Rio do Janeiro, Rio de Janeiro (UFRJ); Museum of Zoology of the State University of Feira de Santana, Feira de Santana (UEFS). Comparative material is listed in Mattos et al. (2015). The distribution map was generated using QGIS Geographic Information System, Open Source Geospatial Foundation Project, and the information of this map was based on our examined material and data provided by Mattos et al. 2015. Specimens were euthanized by immersion in a buffered solution of tricaine methane sulphonate (MS-222) at a concentration of 250 mg/L, for a period of 10 minutes, following the guidelines of the Journal of the American Veterinary Medical Association (AVMA Guidelines) (Leary et al. 2013) and European Commission DGXI consensus for fish euthanasia (Close et al. 1996, 1997). Tissue specimens for molecular analysis (DNA) were fixed and preserved in absolute ethanol just after collection.

Species delimitation

The species delimitation methodology followed in this study aims to fulfil goals of integrative taxonomy. The character-based methodology for species delimitation was the Population Aggregation Analysis. It employs a unique combination of morphological character states to diagnose species. This method of species delimitation was formally described by Davis and Nixon (1992).

The PAA applied for molecular data in this study aimed the unique substitution nucleotide for each gene analysed (Costa and Amorim 2014, Costa et. al. 2014, Costa et. al. 2017). The character-state optimization among the '*G.*' *brasiliensis* species group and another included genus were performed using PAUP4 by most parsimonious reconstruction method (Swofford 1993). The relative numeric position was determined for each transformation through sequence alignment with the complete mitochondrial genome of *Astronotus ocellatus* (Agassiz, 1831) (Mabuchi et al. 2007). Plesiomorphic state for each species was presented before arrow and apomorphic state after the arrow.

The tree-based approach used for molecular data was proposed by Wiens and Penkrot (2002), in which species are delimited through well supported clades of haplotypes with concordant geographic distribution. The significance of the branches for species delimitation was evaluated by the support values, bootstrap values equal or higher than 70% as significant (Hillis and Bull 1993) and posterior probability of the branches values equal or higher than 0.95 as significant (Alfaro and Holder 2006).

DNA extraction, amplification and sequencing

Total genomic DNA was extracted from muscular tissue of the right side of the caudal peduncle using the DNeasy Blood & Tissue Kit (Qiagen). Sequence fragments of cytochrome b (CYTB) with 1,100 bp and cytochrome c oxidase I (COI) with 680 bp were obtained. To amplify these DNA fragments, we used primers available in the literature (Farias et al. 2001). Polymerase chain reaction (PCR) was performed in 50 µl reaction mixtures containing 5× Green GoTaq Reaction Buffer (Promega), 3.2 mM MgCl2, 1 µM of each primer, 75 ng of total genomic DNA, 0.2 mM of each dNTP and 1U of Taq polymerase. The thermocycling profile was: (1) 1 cycle of 4 minutes

at 95 °C; (2) 35 cycles of 1 minute at 92 °C, 1 minute at 48–50 °C and 1 minute at 72 °C; and (3) 1 cycle of 4 minutes at 72 °C. Negative controls were used to check DNA contamination in all PCR reactions. Amplified PCR products were purified using the Wizard SV Gel and PCR Clean-Up System (Promega). Sequencing reactions were made using the BigDye Terminator Cycle Sequencing Mix (Applied Biosystems). Cycle sequencing reactions were performed in 10 µl reaction volumes containing 1 µl BigDye 2.5, 1.55 µl 5× sequencing buffer (Applied Biosystems), 2 µl of the amplified products (10–40 ng), and 2 µM of primer. The thermocycling profile was 30 cycles of 10 seconds at 96 °C, 5 seconds at 54 °C and 4 minutes at 60 °C. The sequencing reactions were purified, and the samples were run on an ABI 3130 Genetic Analyzer.

Phylogenetics analysis

Sequences were edited using MEGA 6.0 (Tamura et al. 2013) and aligned using ClustalW (Chenna et al. 2003); subsequently sequences were translated into amino acids residues to verify the absence of premature stop codons or indels. The best-fit model of sequence evolution was calculated by JModelTest 2.1.7 (Darriba et al. 2012), which provided the same evolutive model for both genes fragments, General Time Reversible (Nei and Kumar 2000), with 5 rate categories and by assuming that a certain fraction of sites is evolutionarily invariable.

Phylogenetic analyses were performed using PAUP4 for maximum parsimony (MP), MrBayes v.3.2.1 (Ronquist et al. 2012) for Bayesian inference (BI) and GARLI v.2.0 (Zwickl 2006) for maximum likelihood (ML) methods for the mitochondrial concatenated dataset. MP was performed with branch-and-bound search algorithm; and tree branch support was given by bootstrap analysis, using a heuristic search with 1000 replicates and the same settings used in the MP search. ML searches for the best tree were performed in five independent replications with at least 10,000 generations, since no topology improvement was observed by adding more generations. ML tree branch support was calculated with 1000 non-parametric bootstrap replicates (Felsenstein 1985). BI was performed with the following settings: two Markov chain Monte Carlo (MCMC) runs of four chains each for 30 million generations, a sampling frequency of 1000. All parameters between partitions except topology and branch lengths were unlinked. The convergence of the MCMC chains were graphically assessed by evaluating the stationary phase of the chains using Tracer v. 1.5 (Rambaut et al. 2014). Consensus topology and posterior probabilities were obtained after applying a burn-in of the first 25% of the generated trees.

The molecular data matrix includes 27 terminal taxa of in-group terminals representing twelve populations scattered throughout the eastern range of the '*G.*' *brasiliensis* specie group distribution, including topotypes of all species. List of ingroup specimens and respective Gen-Bank accession numbers are shown in Table 1. Outgroups comprise seven species of five Geophagini genera closely related to the '*Geophagus*' *brasiliensis* species group (Smith et al. 2008, López-Fernández et al. 2010). Additional sequences of CYTB and COI for the following out-group taxa were obtained from GenBank (accession number): *Biotodoma wavrini* (Gosse, 1963) (GU736928/ EU888075); *Geophagus steindachneri* Eigenmann & Hildebrand, 1922 (AF370660/ DQ119217); *Geophagus surinamensis* (Bloch, 1791) (GU736944/ JN026709); *Gymnogeophagus gymnogenys* (Hensel, 1870) (GU736950/ EU888086); *Mikrogeophagus altispinosus* (Haseman, 1911) (GU736953/ EU888090); and *Mikrogeophagus ramirezi* (Myers & Harry, 1948) (AF370664/ KU568932.1).

Table 1. Vouchers and GenBank accession numbers for new sequenced material of *Geophagus*.

Species	DNA sample voucher	GeneBank accesion number		GenSeq Nomenclature
		COI	CYTB	
G. brasiliensis	UFRJ 8365.1	MH538060	KT373984	genseq-3
	UFRJ 8365.2	MH538061	KT373985	genseq-3
	UFRJ 7925.1	MH538062	KT373988	genseq-4
	UFRJ 8251.1	MH538063	KT373987	genseq-4
	UFRJ 7738.2	MH538064	KT373986	genseq-4
G. iporangensis	UFRJ 8628.1	MH538065	MH538045	genseq-4
	UFRJ 8628.2	MH538066	MH538046	genseq-4
	UFRJ 8617.1	MH538067	MH538047	genseq-3
	UFRJ 8617.2	MH538068	MH538048	genseq-3
G. rufomarginatus	URFJ 9518.1	MH538069	MH538049	genseq-2
	URFJ 9519.1	MH538070	MH538050	genseq-3
	URFJ 9519.2	MH538071	MH538051	genseq-3
	URFJ 1103.1	MH538072	MH538052	genseq-2
	URFJ 1103.2	MH538073	MH538053	genseq-2
G. itapicuruensis	UFRJ 9442.1	MH538074	KT374000	genseq-3
	UFRJ 9442.2	MH538075	KT374001	genseq-3
	UFRJ 9442.3	MH538076	KT374002	genseq-3
	UFRJ 9442.4	MH538077	KT374003	genseq-3
G. multiocellus	UFRJ 8254.1	MH538078	MH538057	genseq-2
	UFRJ 8254.2	MH538079	MH538058	genseq-2
	UFRJ 8254.3	MH538080	MH538059	genseq-2
G. santosi	UFRJ 9998.1	MH538081	MH538054	genseq-2
	UFRJ 9998.2	MH538082	MH538055	genseq-2
	UFRJ 9998.3	MH538083	MH538056	genseq-2
G. diamantinensis	UFRJ 8245.1	MH538084	KT373992	genseq-2
	UFRJ 8245.2	MH538085	KT373993	genseq-2
	UFRJ 8245.3	MH538086	KT373994	genseq-2
	UFRJ 8245.4	MH538087	KT373995	genseq-2
G. obscurus	UFRJ 9440.1	MH538088	KT373998	genseq-3
	UFRJ 9440.2	MH538089	KT373999	genseq-3
	UFRJ 10026.1	MH538090	KT373996	genseq-3
	UFRJ 10026.1	MH538091	KT373997	genseq-3

Results

The MP, ML and IB analyses generated trees with the same topology (Fig. 1). All species of the '*G.*' *brasiliensis* species group were recovered as exclusive lineages:

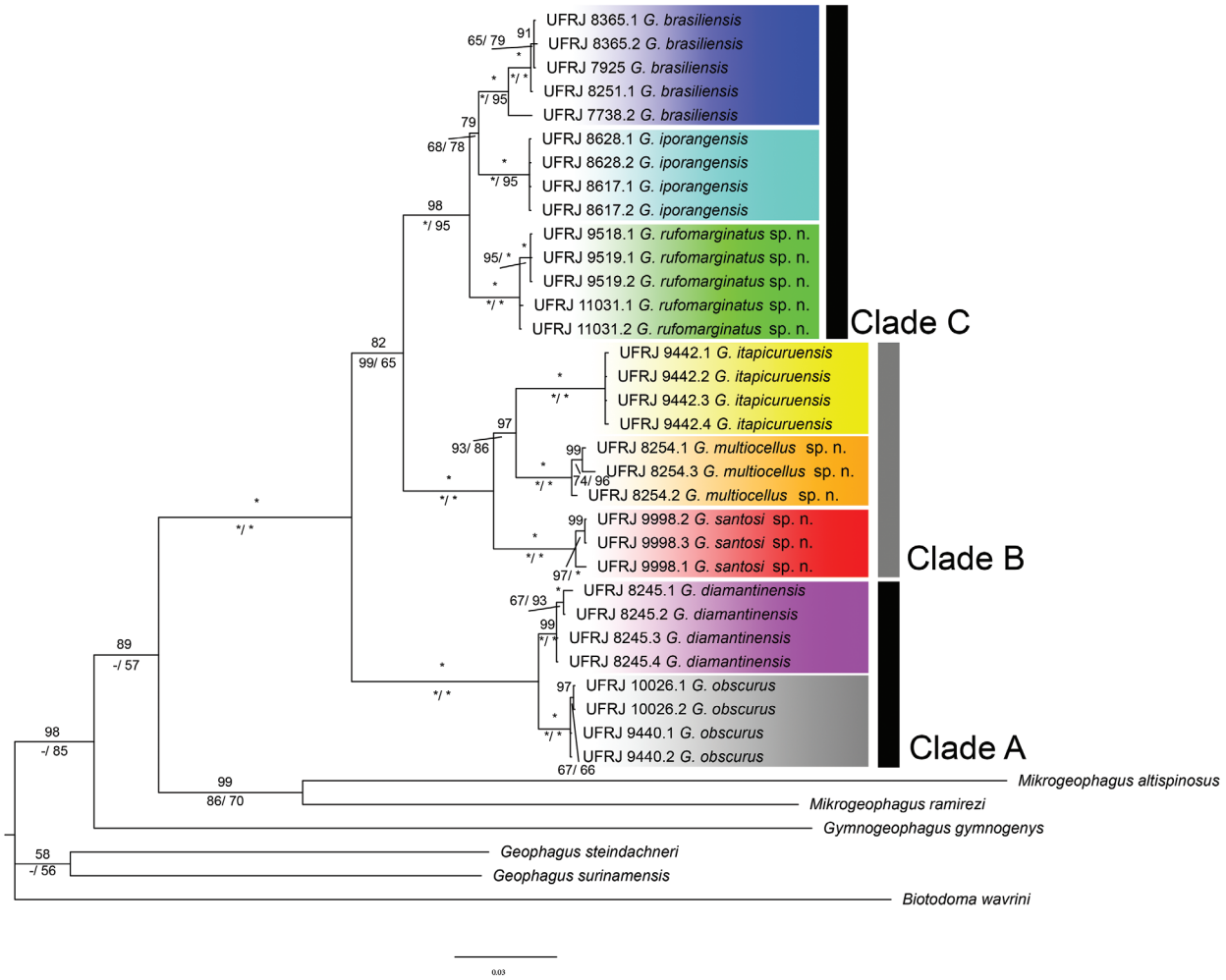

Figure 1. Tree topology estimated by Bayesian inference analysis for the '*Geophagus*' *brasiliensis* species group. Numbers before terminal species names are voucher numbers. Numbers above branches indicates Bayesian posterior probabilities and below bootstrap values of the Maximum Parsimony and Maximum Likelihood analyses, respectively, separated by bar. Dashes indicate values below 50 and asterisks indicate maximum support values.

G. brasiliensis, *G. iporangensis*, *G. itapicuruensis*, *G. obscurus* and *G. diamantinensis*. Additionally, three new species were congruently supported as exclusive lineages for the Rio de Contas, Rio Buranhém and Rio Mariana basins. The PAA analyses also supported the recognition of all the species mentioned above. The three new species were also supported by unique colour patterns and unique nucleotide substitutions.

The *'G.'* *brasiliensis* species group was recovered as a monophyletic group. Three main strongly supported clades were recovered within the *'G.'* *brasiliensis* species group: the clade A endemic to the Rio Paraguaçu Basin, comprising *G. obscurus* and *G. diamantinensis*; the clade B endemic to an area encompassing the Rio de Contas, Rio Itapicuru, and Rio Mariana basins and comprising *G. itapicuruensis* and two new species; and The clade C geographically widespread clade comprising *G. brasiliensis*, *G. iporangensis* and the new species from the Rio Buranhém Basin.

Geophagus rufomarginatus sp. n.

http://zoobank.org/E402678B-DABD-4DF3-B013-84D00A71F5C6
Fig. 2, Table 2

Material. *Holotype.* UFRJ 9994, 97.8 mm SL; Brazil, Bahia state: Porto Seguro municipality: small stream crossing the road BA-001, Rio Buranhém Basin, 16°26'17"S, 39°10'47"W, altitude about 10 m asl; A. M. Katz, F. R. Pereira and J. L. O. Mattos, 20 July 2016.

Paratypes. UFRJ 11198, 6, 89.5–104.1 mm SL, 1, 94.3 mm SL (d&c); UFRJ 11031, 2, 15.9–41.6 mm SL (DNA); CICCAA 01378, 2, 94.3–97,6 mm SL; collected with holotype. UFRJ 9741, 1, 103.5 mm SL; UFRJ 9518, 7, 20.4–40.9 mm SL; Brazil, Bahia state: Eunápolis municipality: Rio Buranhém crossing the road BR-101, Rio Buranhém Basin, 16°24'47"S, 39°35'14"W, altitude about 65 m asl; F. R. Pereira and F. P. Ottoni, 23 June 2013. UFRJ 9519, 6, 17.3–40.7 mm SL (DNA); Brazil, Bahia state: Rio Buranhém under BA-001 road bridge, between

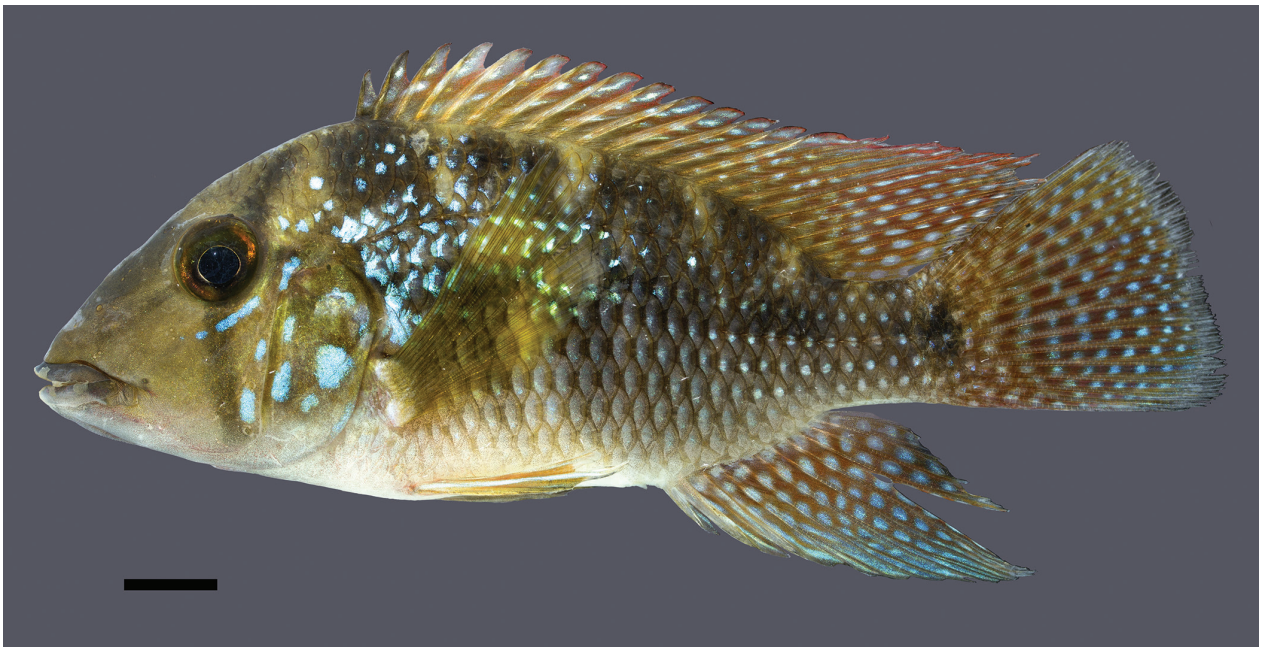

Figure 2. *Geophagus rufomarginatus*, UFRJ 9994, holotype, 96.8 mm SL; Brazil: Bahia: Rio Buranhém Basin. Scale bar 10 mm. Photograph by J.L.O. Mattos.

the towns of Porto Seguro and Trancoso, Rio Buranhém Basin, 16°23'32"S, 39°17'08"W, altitude about 20 m asl; F. R. Pereira and F. P. Ottoni, 24 June 2013.

Diagnosis. *eophagus rufomarginatus* is distinguished from all other species of '*G.*' *brasiliensis* group by having: dorsal-fin lappets with red edges (vs. grey or dark brown), presence of longitudinal series of small light blue spots between anal-fin spines and rays (vs. never this pattern), and non-denticulated gill-rakers (vs. denticulated). In addition, it is distinguished from all other species of the '*G.*' *brasiliensis* species group, except *G. obscurus* and *G. santosi*, by having an oblique iridescent blue zone between the humeral region and the anterior portion of the dorsal-fin base (vs. iridescent blue zone absent). It is also distinguished from *G. diamantinensis* by the absence of a dark brown mark on the humeral region (vs. presence); presence of iridescent blue to green spots on the opercular region (vs. whole opercular region golden); and absence of a horizontal dark brown band on the snout (vs. presence).

In addition, *G. rufomarginatus* is also distinguished from all other species of '*G.*' *brasiliensis* group by 13 unique nucleotide substitutions: COI 285 (T > C), COI 330 (T > C), COI 333 (T > C), COI 591 (A > C), COI 642 (C > T), CYTB 60 (C > T), CYTB 129 (C > T), CYTB 186 (C > T), CYTB 309 (C > T), CYTB 324 (A > G), CYTB 886 (T > C), CYTB 906 (A > G), CYTB 958 (C > T); it is similar to *G. iporangensis* and *G. brasiliensis* and distinguished from all other species of the '*G.*' *brasiliensis* group by four unique nucleotide substitutions: COI 700 (T > C), CYTB 165 (C > T), CYTB 582 (A > G), CYTB 1078 (A > C).

Description. Morphometric data appear in Table 2. Medium sized species, largest specimen examined 104.2 mm SL. Body relatively slender and compressed. Dorsal profile slightly convex on head, convex from nape to end of dorsal-fin base, approximately straight on caudal peduncle; no adipose nuchal protuberance. Ventral profile straight to slightly convex from lower jaw to pelvic-fin insertion, slightly convex between belly and end of anal-fin base, nearly straight on caudal peduncle. Caudal peduncle approximately as deeper as long. Greatest body depth at level of first dorsal-fin spine. Snout moderately pointed; nostrils located between tip of snout and anterior margin of orbit. Mouth subterminal, distal tip of maxilla not reaching vertical through anterior margin of orbit. Lower lip fold moderately deep. Lower jaw slightly shorter than upper one. Eye near dorsal profile of head. Opercle not serrated.

Insertion of first dorsal-fin spine slightly anterior to vertical line through posterior-most margin of opercle. Tip of dorsal-fin pointed, reaching 30–90% of caudal-fin length, shorter and rounded in specimens 40.0 mm SL or smaller. Tip of anal fin pointed, reaching 30–50% of caudal-fin length, shorter and rounded in specimens 43.0 mm SL or smaller. Caudal fin subtruncate. Pectoral fin trapezoidal with rounded extremity, posterior margin posteriorly surpassing flank blotch. Tip of pelvic-fin pointed, short, reaching insertion of 1st anal-fin spine in larger specimens, shorter and rounded in specimens 50.0 mm SL or smaller, reaching between urogenital papilla and insertion of first anal-fin spine. Pelvic-fin filaments absent. Anal-fin origin at vertical between insertion of 13th dorsal-fin spine and 1st dorsal- fin ray. Dorsal fin XIV + 12–13 (23); anal fin III + 9–10 (23); pectoral-fin rays 15 (23); pelvic fin I + 5 (26). Caudal-fin rays iv + 16 + iv (5).

Table 2. Morphometric data of *G. rufomarginatus*. H, holotype; SD, standard deviation. Values of holotype included in range.

	H	range (n=8)	mean	SD
Standard length (mm)	96.83	89.5–104.1	–	–
Percentage of standard length				
Body depth	43.7	42.7–44.6	43.4	0.7
Predorsal length	47.3	43.7–47.3	45.8	1.3
Dorsal-fin base length	55.9	55.4–57.7	56.2	0.7
Last dorsal-fin spine length	15.3	15.1–16.7	15.8	0.6
Prepelvic length	43.4	41.6–44.5	43.1	1.0
Pelvic-fin length	34.9	31.7–34.9	32.9	1.2
Pelvic-fin spine length	16.2	15.0–16.8	15.9	0.7
Pectoral-fin length	31.5	31.4–32.8	32.1	0.5
Anal-fin base length	17.9	14.5–20.1	18.2	1.8
Last anal-fin spine length	15.3	14.5–16.0	15.5	0.5
Caudal peduncle length	13.5	13.5–17.3	14.8	1.4
Caudal peduncle depth	14.1	12.9–14.8	14.0	0.6
Head length	40.2	35.2–41.6	39.4	2.1
Percentage of head length				
Snout length	50	46–52	49.4	2.3
Preorbital depth	69	64–69	67.6	1.6
Head width	46	46–50	48.1	1.5
Head depth	89	87–93	90.5	2.3
Orbital diameter	23	23–27	24.4	1.3
Interorbital width	26	26–31	28.5	1.8
Upper jaw length	35	31–35	33.5	1.4
Lower jaw length	30	28–30	29.2	0.9

Side of head covered with cycloid scales, ventral surface of head and snout without scales. Chest, trunk and caudal peduncle covered with ctenoid scales. Scales on head smaller than scales on chest and flank. Dorsal and anal fins without scales. About one fourth of caudal fin covered with small, delicate scales. Two scale rows between lateral lines. Scales of dorsal-fin origin row 5; scales of anal-fin origin row 6; longitudinal series of scales 26; cheek scale row 5; upper lateral line scales 18, lower lateral line scales 11 + 2; circum-peduncular scale rows 16.

Premaxillary teeth conical, hyaline with red tip, slightly curved posteriorly; one regular outer row of teeth, increasing in size on symphysis; proximal teeth smaller and irregularly arranged. Dentary teeth with similar arrangement, but slightly smaller. Five branchiostegal rays. Urohyal with strong anterior constriction. Gill-rakers on first branchial arch: first ceratobranchial 12, articulation 1, first epibranchial 9. Ceratobranchial rakers short, blunt and denticulated, except on fourth ceratobranchial proximal margin and fifth ceratobranchial distal margin, conical and non-denticulated. Anterior teeth of third pharyngobranchial and fifth ceratobranchial small, thin and slightly curved anteriorly, proximal posterior teeth large, robust and circular in cross section. Distal posterior teeth of the fifth ceratobranchial laterally compressed and with one or two cuspids. Five dentigerous plate on fourth pharyngobranchial. Fifth ceratobranchial subtriangular, with concave posterior margin. One supraneural. Proximal radial of dorsal fin 25 + 1; proximal radial of anal fin 10 + 1; pleural ribs 13, epipleural ribs 12; vertebrae 14 + 14.

Colouration in life. Flank yellowish brown with seven broad dark brown bars and one dark brown longitudinal stripe; dark brown bars and stripe often overlapped and without visible limits in live specimens, conspicuously delimited in preserved specimens. Pale blue iridescence on anteroventral portion of flank and small metallic blue dots on centre of scales of middle portion of flank and caudal peduncle. Rounded dark brown spot on fifth trunk bar, sometimes inconspicuous in live specimens; similar and smaller spot on middle of posterior portion of caudal peduncle. Oblique iridescent blue zone between humeral region and anterior portion of dorsal-fin base. Dorsum yellowish brown, chest and belly pinkish white.

Head greyish brown with ventral region lighter, branchiostegal region light red. Infra-orbital area with small metallic blue dots, most of them coalesced. Opercular region background colour yellowish brown. Opercular and temporal regions with few elliptical, small and large metallic blue spots spread through opercle. Iris golden brown, with dark brown bar through orbit not aligned to any portion of supra-orbital and infra-orbital stripes. Dark brown supra-orbital stripe extending from nape to posterodorsal margin of orbit, and dark brown infra-orbital stripe, approximately vertical, running between ventral margin of orbit and preopercle angle. Dorsal fin brownish yellow on basal portion, becoming reddish orange on distal and posterior portions, with metallic blue dots aligned between rays; marginal lappets with red edges; dark brown pigmentation concentrated at first two dorsal-fin spines. Anal fin reddish orange with small metallic blue spots, to brownish yellow with metallic blue lines parallel to rays and spine on anteriormost portion of fin; intense blue iridescence on distal portion of anal fin. Caudal fin reddish orange, to brownish yellow on posterodorsal corner, with small metallic blue rounded dots, vertically coalesced to form metallic blue bars on anterior portion; posterior margin dark bluish grey. Pectoral fin yellowish hyaline. Pelvic-fin spine light yellowish brown, anterior pelvic-fin rays light yellowish brown with metallic bluish stripes parallel to rays, region around last rays hyaline.

Colouration in alcohol. Similar to colouration in life, except for metallic marks becoming dark brown on flank and light grey on fins; red and dark brown pigmentation fainted.

Distribution. Known only from the middle and lower sections of the Rio Buranhém Basin, at altitudes of about 65 m above sea level or less, Bahia state, northeast Brazil (Fig. 3).

Etymology. From the Latin *marginatus* (edge, border, margin) and *rufo* (red), an allusion to the colour pattern in life of the dorsal-fin lappets.

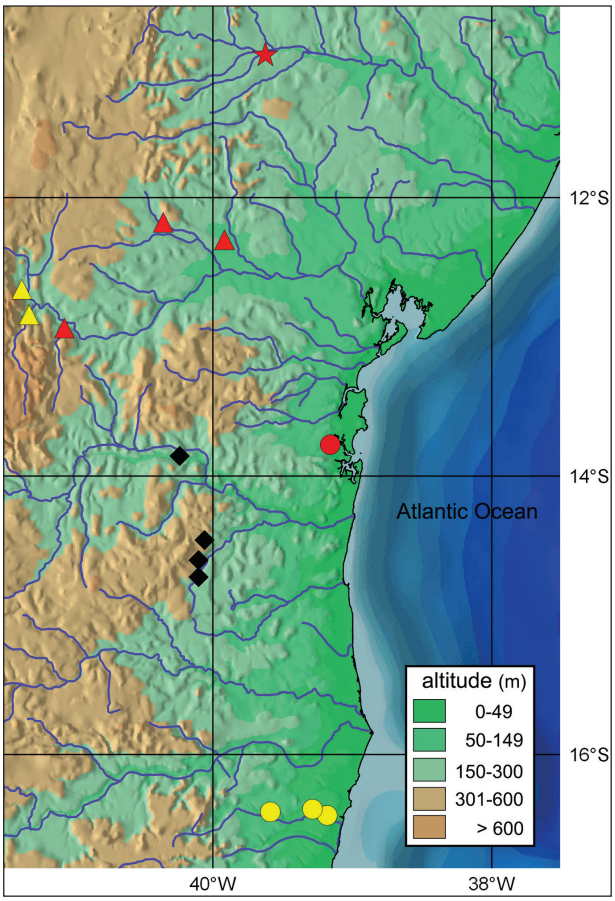

Figure 3. Geographical distribution of the '*Geophagus*' *brasiliensis* species group in northeast Brazil: red star, *G. itapicuruensis*; red triangle, *G. obscurus*; yellow triangle, *G. diamantinensis*; red circle, *G. santosi*; black diamond, *G. multiocellus*; yellow circle, *G. rufomarginatus*. Raw data set source was obtained from Natural Earth public domain (http://www.naturalearthdata.com).

Geophagus multiocellus sp. n.

http://zoobank.org/873C4147-778E-4798-A8C8-FD89EE459969
Figs 4, 5, Table 3

Material. *Holotype.* UFRJ 11764, 101.4 mm SL; Brazil: Bahia state: Iguaí municipality: Guaíra balneary, Rio Cambiriba, Rio Gongogi drainage, Rio de Contas Basin, 14º36′17″ S 40º06′09″ W, altitude about 345 m asl; W. J. E. M. Costa et. al., 18 June 2011.

Paratypes. UFRJ 8217, 6, 57.4–102.9 mm SL; UFRJ 8254, 5, 26.5–41.9 mm SL (DNA); CICCAA 01379, 2, 78.9–82.7 mm SL; collected with holotype. UFRJ 8222, 5, 63.3–68.4 mm SL; UFRJ 8246, 2, 35.1–35.7 mm SL (DNA); Brazil: Bahia state: Nova Canaã municipality: small stream crossing the road BA-262, between the villages of Nova Canãa and Poções, Rio de Contas Basin, 14º43′33″ S 40º14′17″ W, altitude about 545 m asl; W. J. E. M. Costa et. al., 18 June 2011. MNRJ32263, 5, 7.8–9.6 mm SL, 1, 8.2 mm SL (C&S); Brazil: Bahia state: Poções municipality, stream of Rio Valentim drainage, Rio de Contas River Basin, 14°27'38"S, 40°03'34"W (approx.), altitude about 365 m asl; M. Cetra and M. Trindade. 02 February 2007. MNRJ 22302, 47, 6.2–101.1 mm SL, 2, 7.2–7.9 mm SL (C&S); Brazil; Bahia state: Jequié municipality: Rio de Contas Basin, 13°51'22"S, 40°4'58"W (approx.), altitude about 270 m asl; P. A. Buckup, A. T. Aranda and F. A. G. Melo. 12 August 2001.

Diagnosis. *Geophagus multiocellus* is distinguished from all other species of the '*G.*' *brasiliensis* group by having small pale blue spots with minute bright blue dots on its centre, often vertically coalesced to form short bars on the caudal fin (vs. never a similar pattern). In addition, it is distinguished from *G. rufomarginatus*, *G. obscurus* and *G. santosi* by the absence of an oblique iridescent blue zone between humeral region and anterior portion of dorsal-fin base (vs. iridescent blue zone present); from *G. rufomarginatus* by having dorsal-fin lappets with grey or dark brown edges (vs. red); presence of denticles on gill-rakers of the first branchial arch (vs. absence); absence of longitudinal series of small light blue spots between anal-fin spines and rays (vs. presence); from *G. santosi* by having blue bands crossing anal-fin rays (vs. blue bands parallel to fin rays); from *G. itapicuruensis* by having XIV dorsal-fin spines (vs. XIII); lateral spot rounded (vs. elliptical); absence of a horizontal dark brown band on snout (vs. presence); and from *G. brasiliensis* by having longitudinal blue bands crossing the anal-fin rays (vs. transversal blue bands crossing the anal-fin rays); mouth subterminal (vs. subdorsal).

Geophagus multiocellus is also distinguished from all other species of the '*G.*' *brasiliensis* group by ten unique nucleotide substitutions: COI 279 (C > T), COI 363 (G > A), CYTB 30 (C > T), CYTB 147 (A > G), CYTB 195 (C > T), CYTB 841 (C > T), CYTB 873 (C > T), CYTB 945 (A > G), CYTB 1014 (T > C) CYTB 1023 (A > G); it is similar to *G. itapicuruensis* and *G. santosi* and distinguished from all other species of the '*G.*' *brasiliensis* group by three unique nucleotide substitutions: COI 678 (A > G), CYTB 114 (A > G), CYTB 927 (A > G).

Description. Morphometric data appear in Table 3. Medium sized species, largest specimen examined 102.9 mm SL. Body relatively slender and compressed. Dorsal profile slightly convex on head, convex from nape to end of dorsal-fin base, approximately straight on caudal peduncle; no adipose nuchal protuberance. Ventral profile convex from lower jaw to pelvic-fin insertion, nearly straight between belly and insertion of first anal-fin spine, about straight on anal-fin base, gently concave on caudal peduncle. Caudal peduncle approximately as deeper as long. Greatest body depth slightly anterior to first dorsal-fin spine insertion. Snout moderately pointed; nostrils located between tip of snout and anterior margin of orbit. Mouth subterminal, distal tip of maxilla not reaching vertical through anterior margin of orbit. Lower lip fold

Figure 4. *Geophagus multiocellus*, UFRJ 11764, holotype, 101.4 mm SL; Brazil: Bahia: Rio de Contas Basin. Scale bar 10 mm. Photograph by J.L.O. Mattos.

moderately deep. Lower jaw slightly shorter than upper one. Eye near dorsal profile of head. Opercle not serrated.

Insertion of first dorsal-fin spine slightly anterior to vertical line through posterior-most margin of opercular series. Tip of dorsal fin pointed, reaching 35–50% of caudal-fin length, shorter and rounded in specimens 41.0 mm SL or smaller. Tip of anal fin pointed, reaching 20–50% of caudal-fin length, shorter and rounded in specimens 41.0 mm SL or smaller. Caudal fin subtruncate. Pectoral fin trapezoidal with rounded extremity, posterior margin posteriorly reaching vertical through posterior margin of flank blotch.

Tip of pelvic fin pointed, short, reaching insertion of 3rd anal-fin spine in larger specimens; shorter and rounded in specimens 50.0 mm SL or smaller, reaching between urogenital papilla and insertion of first anal-fin spine. Pelvic-fin filaments absent. Anal-fin origin at vertical between insertion of 13th dorsal-fin spine and 1st dorsal-fin ray. Dorsal fin XIV–XV + 11–12 (26); anal fin III + 8–9 (26); pectoral-fin rays 14–15 (26); pelvic fin I + 5 (26). Caudal-fin rays vi + 16 + iii (4).

Side of head covered with cycloid scales, ventral surface of head and snout without scales. Chest, trunk and caudal peduncle covered with ctenoid scales. Scales on head smaller than scales on chest and flank. Dorsal and anal fins without scales. About one fourth of caudal fin covered with small delicate scales. Two scale rows between lateral lines. Scales of dorsal-fin origin row 5; scales of anal-fin origin row 6; longitudinal series of scales 26; cheek scale row 5; upper lateral line scales 18, lower lateral line scales 11 + 2; circum-peduncular scale rows 16.

Premaxillary teeth conical, hyaline with red tip, slightly curved posteriorly; one regular, outer row of teeth, increasing in size on symphysis; proximal teeth smaller and irregularly arranged. Dentary teeth with similar arrangement, but slightly smaller. Five branchiostegal rays. Urohyal with strong anterior constriction. Gill-rakers on first branchial arch: first ceratobranchial 11, articulation 1, first epibranchial 8. Ceratobranchial rakers short, blunt and denticulated, except on fourth ceratobranchial proximal margin and fifth ceratobranchial distal margin, conical and non-denticulated. Anterior teeth of third pharyngobranchial and fifth ceratobranchial small, thin and slightly curved anteriorly, posterior teeth larger, robust and circular in cross section. Distal posterior teeth of the fifth ceratobranchial laterally compressed and with one or two cuspids. Five or six dentigerous plate on fourth pharyngobranchial, with three or four fused. Fifth ceratobranchial subtriangular, with concave posterior margin. One supraneural. Proximal radial of dorsal fin 25 + 1; proximal radial of anal fin 8 + 1; pleural ribs 12; epipleural ribs 12; vertebrae 14 + 14.

Colouration in life. Flank greyish brown with seven broad dark brown bars and one dark brown longitudinal stripe; dark brown bars and stripe often overlapped and without visible limits in live specimens, conspicuously delimited in preserved specimens. Longitudinal rows of golden spots on ventral part of flank, between pectoral-fin insertion and caudal-fin base; spots approximately occupying ventral half-length of scales. Rounded dark brown spot on fifth trunk bar, similar and smaller spot on middle of caudal peduncle. Humeral region with three metallic blue spots arranged in oblique row. Dorsum greyish brown, chest and belly greyish white.

Head greyish brown, ventral region lighter, branchiostegal region greyish white. Infra-orbital area with oblique row of small metallic greenish blue spots. Opercular region background colour greyish brown. Absence or up to five small elliptical metallic greenish blue spots spread through opercle. Iris golden brown, with greenish blue iridescence on anterior and posterior portions, and dark brown bar through orbit aligned with sub-orbit-

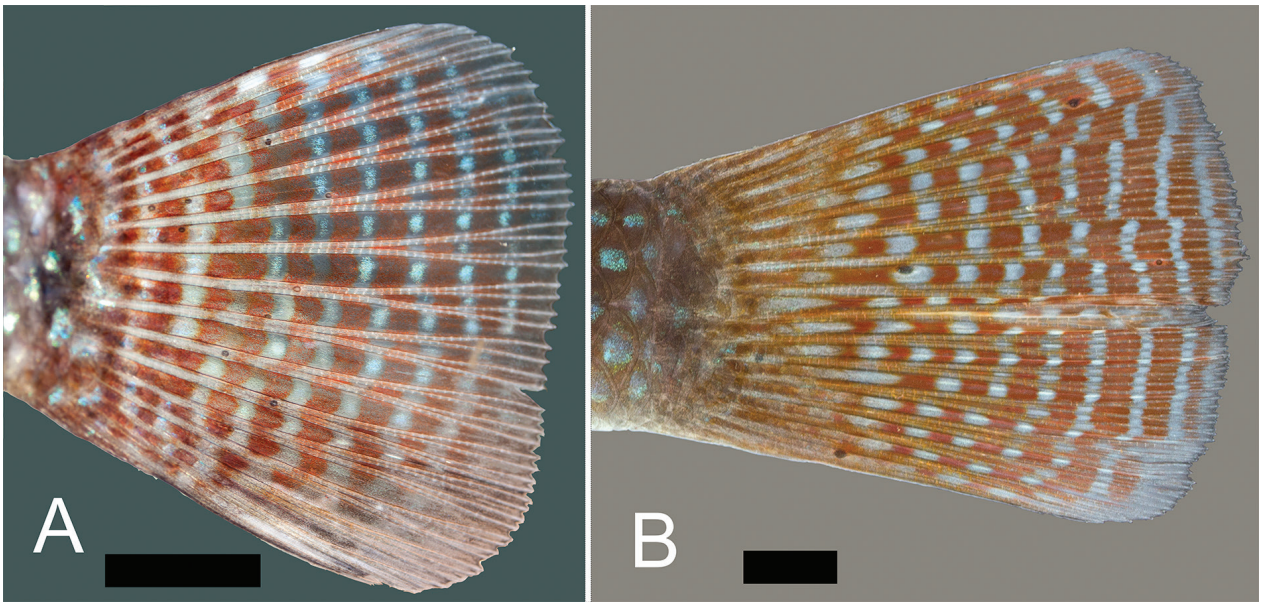

Figure 5. Caudal fin colour pattern. **A** *Geophagus multiocellus*, UFRJ 8217, topotype. **B** *Geophagus santosi*, UFRJ 9998, topotype. Scale bar 10 mm. Photographs by J.L.O. Mattos.

Table 3. Morphometric data of *G. multiocellus*. H, holotype; SD, standard deviation. Values of holotype included in range.

	H	range (n=10)	mean	SD
Standard length (mm)	101.0	57.4-102.9	–	–
Percentage of standard length				
Body depth	40.8	39.6-41.2	40.3	0.5
Predorsal length	45.5	42.4-47.4	45.0	1.9
Dorsal-fin base length	52.8	52.5-56.7	53.9	1.6
Last dorsal-fin spine length	14.1	12.5-14.4	13.6	0.6
Prepelvic length	43.4	42.1-44.6	43.4	1.0
Pelvic-fin length	29.3	26.2-44.3	30.2	5.4
Pelvic-fin spine length	12.5	12.1-15.2	13.4	1.0
Pectoral-fin length	31.1	29.8-32.5	31.3	0.7
Anal-fin base length	17.5	16.6-18.4	17.4	0.6
Last anal-fin spine length	14.0	11.8-14.4	13.5	0.8
Caudal peduncle length	12.4	10.7-14.2	12.8	1.0
Caudal peduncle depth	13.5	13.2-14.6	13.9	0.5
Head length	38.0	35.1-38.4	37.1	1.1
Percentage of head length				
Snout length	56	48-56	51.4	3.1
Preorbital depth	70	63-72	67.6	3.3
Head width	55	52-58	55.2	1.8
Head depth	91	87-98	90.6	2.9
Orbital diameter	24	24-31	27.1	1.9
Interorbital width	31	28-32	29.9	1.3
Upper jaw length	35	30-37	33.6	1.6
Lower jaw length	27	25-31	27.5	2.6

al stripe. Pale brown supra-orbital stripe extending from dorsal profile to postero-dorsal margin of orbit, and dark brown infra-orbital stripe, approximately vertical, running from ventral margin of orbit to sub-opercle. Dorsal fin brownish red; anterior portion with short, oblique metallic blue stripes, posterior region with transverse rows of small pale blue spots; dark brown pigmentation concentrated at first two dorsal-fin spines and distal half of third spine. Anal fin brownish red, with oblique metallic blue stripes, posterior-most region with longitudinal rows of small, elongated pale blue spots. Caudal fin brownish red with small pale blue spots with minute bright blue dots on its centre, often vertically coalesced to form short bars. Pectoral fin pale yellowish hyaline. Pelvic-fin spine light yellowish brown, anterior pelvic-fin rays light yellowish brown with metallic bluish stripes parallel to rays, region around last rays hyaline.

Colouration in alcohol. Similar to colouration in life, except for metallic blue marks becoming dark brown on flank and light grey on fins; red and dark brown pigmentation faded.

Distribution. Known only from the middle section of the Rio de Contas Basin, in altitudes between about 270 and 545 m above sea level, Bahia state, northeast Brazil (Fig. 3).

Etymology. From the Latin *multum* (several) and *ocellus* (little eyes, jewels), an allusion to the presence of small pale blue spots with minute bright blue dots on its centre on the caudal fin.

Geophagus santosi sp. n.

http://zoobank.org/AEAE1FF0-0A2C-4F98-B9C3-8F5EBAC8AA6D
Figs 5, 6, Table 4

Material. *Holotype.* UFRJ 11765, 99.7 mm SL; Brazil: Bahia state: Ituberá municipality: Rio Mariana upstream of Cachoeira da Pancada, Área de Proteção Ambiental Michelin, 13°46’32"S, 39°09’29"W, altitude about 15 m asl; W. J. E. M. Costa et. al., 21 February 2014.

Paratypes. UFRJ 9998, 3, 92.0-113.4 mm SL (DNA); CICCAA 01380, 1, 99.5 mm SL; collected with holotype. UEFS 10336, 2, 78.1–94.4 mm SL, 1, 78.06 mm SL (C&S); UEFS 10519, 1, 115.0 mm SL, 1, 58.2 mm SL (C&S); UEFS 11585, 8, 69.5–148.4 mm SL; UEFS 10098, 7, 114.3–164.3 mm SL; Brazil: Bahia state: Ituberá municipality: Rio Mariana, Michelin APA, approximately 13°46'42"S, 39°09'32"W (approx.), altitude about 15 m asl; A. C. A. Santos et al., October 2007.

Diagnosis. *Geophagus santosi* is distinguished from all other species of the '*G*.' *brasiliensis* group by having dorsal and anal fins with blue stripes parallel to fin rays on their longest portion (vs. transverse blue bands crossing rays or fins with dots), and basal portion of caudal-fin with short, longitudinal bluish-white lines (vs. dots or bars). *Geophagus santosi* is similar to *G. rufomarginatus* and *G. obscurus*, and distinguished from all other species of the '*G*.' *brasiliensis* group, by the presence of an oblique iridescent blue zone between the humeral region and the anterior portion of the dorsal-fin base (vs. absence of an iridescent blue zone). Furthermore, it is also distinguished from *G. obscurus* by the presence of an oblique suborbital row of aligned, small iridescent blue marks, not extending to cheek (vs. suborbital iridescent blue marks irregularly arranged extending to the cheek) and chest profile straight in lateral view (vs. convex); from *G. rufomarginatus* by possessing dorsal-fin lappets with grey or dark brown edge (vs. red) and presence of denticles on the first branchial arch gill-rakers (vs. absence); from *G. itapicuruensis* by having XIV spines on dorsal fin (vs. XIII) and lateral spot rounded (vs. elliptical); from *G. diamantinensis* by the absence of a dark brown mark on the humeral region (vs. presence), absence of a horizontal dark brown band on the snout (vs. presence), and urohyal bone with strong constriction (vs. with gentle anterior constriction); and from *G. brasiliensis* by having a terminal mouth (vs. sub-dorsal).

Geophagus santosi is also distinguished from all species of '*G*.' *brasiliensis* group by 20 unique nucleotide substitutions: COI 143 (T > C), COI 291 (A > G), COI 523 (G > A) COI 564 (T > A) COI 589 (C >T), CYTB 69 (A >G), CYTB 78 (C > T), CYTB 231 (A >G), CYTB 279 (C > T), CYTB 297 (A > C), CYTB 327 (C > T), CYTB 447 (C >A), CYTB 606 (A > G), CYTB 609 (C > T), CYTB 687 (A > G), 735 (C > T), CYTB 801 (T > C), CYTB 852 (T > C), CYTB 915 (A > T), CYTB 1090 (A > G). It is similar to *G. itapicuruensis* and *G. multiocellus* and distinguished from all other species of '*G*.' *brasiliensis* group by three unique nucleotide substitutions: COI 678 (A > G), CYTB 114 (A > G), CYTB 927 (A > G).

Description. Morphometric data appear in Table 4. Medium sized species, largest specimen examined 164.3 mm SL. Body relatively slender and compressed. Dorsal profile slightly convex on head, convex from nape to end of dorsal-fin base, approximately straight on caudal peduncle; no adipose nuchal protuberance. Ventral profile convex from lower jaw to pelvic-fin insertion, gently straight between belly and insertion of first anal-fin spine, nearly straight on anal-fin base, nearly concave on caudal peduncle. Caudal peduncle slightly longer than deep. Greatest body depth at level of first dorsal-fin spine insertion. Snout moderately pointed; nostrils located between tip of snout and anterior margin of orbit. Mouth subterminal, distal tip of maxilla not reaching vertical through anterior margin of orbit. Lower lip fold moderately deep. Lower jaw slightly shorter than upper one. Eye near dorsal profile of head. Opercle not serrated.

Insertion of first dorsal-fin spine slightly anterior or aligned in a vertical line through posterior-most margin of opercular series. Tip of dorsal fin pointed, short, reaching 20–40% of caudal-fin length, even in larger specimens. Tip of anal fin pointed, reaching 20–40% of caudal-fin length. Caudal fin subtruncate. Pectoral fin trapezoidal with rounded extremity, posterior margin posteriorly surpassing flank blotch. Tip of pelvic-fin rounded or pointed, relatively short and reaching between urogenital papilla and insertion of 3rd anal-fin spine. Pelvic-fin filaments absent. Anal-fin origin at vertical between insertion of 13th and 14th dorsal-fin spine. Dorsal fin XIV + 13 (25); anal fin III + 9–10 (25); pectoral-fin rays 15–16 (25); pelvic fin I + 5 (25). Caudal-fin rays vi + 16 + vi (3).

Side of head covered with cycloid scales, ventral surface of head and snout without scales. Chest, trunk and caudal peduncle covered with ctenoid scales. Scales on head smaller than scales on chest and flank. Dorsal and anal fins without scales. About one fifth of caudal fin covered with small delicate scales. Two scale rows between lateral lines. Scales of dorsal-fin origin row 4; scales of anal-fin origin row 5; longitudinal series of scales 26–27; cheek scale row 5; upper lateral line scales 18, lower lateral line scales 9–11 + 2; circum-peduncular scale rows 16.

Premaxillary teeth conical, hyaline with red tip, slightly curved posteriorly; one regular, outer row of teeth, increasing in size on symphysis; proximal teeth smaller and irregularly arranged. Dentary teeth with similar arrangement, but slightly smaller. Five branchiostegal rays. Urohyal with strong anterior constriction. Gill-rakers on first branchial arch: first ceratobranchial 10, articulation 1, first epibranchial 8. Ceratobranchial rakers short, blunt and denticulated, except on fourth ceratobranchial proximal margin and fifth ceratobranchial distal margin, conical and non-denticulated. Anterior teeth of third pharyngobranchial and fifth ceratobranchial small, thin and slightly curved anteriorly, posterior teeth large, robust and circular in cross section. Distal posterior teeth of the fifth ceratobranchial laterally compressed and with one or two cuspids. Five or six dentigerous plate on fourth pharyngobranchial, two of them could merge. Fifth ceratobranchial subtriangular, with concave posterior margin and robust. One supraneural. Proximal radial of dorsal fin 24 + 1; proximal radial of anal fin 10 + 1; pleural ribs 12, epipleural ribs 11; vertebrae 14 + 14.

Colouration in life. Flank orangish brown with seven broad dark brown bars and one dark brown longitudinal

Figure 6. *Geophagus santosi*, UFRJ 11765, holotype, 110.6 mm SL; Brazil: Bahia: Mariana River. Scale bar 10 mm. Photograph by J.L.O. Mattos.

stripe; dark brown bars and stripe often overlapped and without visible limits in live specimens, conspicuously delimited in preserved specimens. Longitudinal rows of metallic light green spots on ventral part of flank, between pectoral-fin insertion and caudal-fin base; spots approximately occupying most scale area. Rounded dark brown spot on fifth trunk bar, similar and smaller spot on middle of caudal peduncle. Oblique iridescent blue zone between humeral region and anterior portion of dorsal-fin base. Dorsum dark orangish brown, chest and belly light pinkish white.

Head side dark orange, ventral surface white; branchiostegal region dark orangish grey. Infra-orbital area with row of four to six small metallic greenish blue dots, sometimes two or three dots coalesced. Opercular region background orangish brown; opercular and temporal regions with scattered metallic greenish blue spots. Iris yellowish brown, with greenish blue iridescence on anterior and posterior portions, and dark brown bar through orbit not aligned to supra-orbital and infra-orbital stripes. Dark brown supra-orbital stripe extending from nape to postero-dorsal margin of orbit, and dark brown infra-orbital stripe, approximately vertical, running between ventral margin of orbit and pre-opercle angle. Dorsal fin pale brown on anterior portion, pale yellow on middle, pale orange on posterior region; oblique series of elongate drop-shaped metallic green spots on anterior two thirds of fin, light blue stripes parallel to fin rays on longest region of fin, and longitudinal rows of rounded light blue spots on posterior portion of fin; dark brown pigmentation most concentrated at first two dorsal-fin spines and distal half of third spine. Anal fin reddish orange, to yellowish orange on basal portion, with longitudinal metallic blue stripes between rays, and metallic blue spots on posterior region. Caudal fin reddish orange with transverse rows of small bluish white spots often coalesced to form narrow bars; basal portion of fin light yellowish orange with short, longitudinal bluish white lines. Pectoral fin pale

Table 4. Morphometric data of *G. santosi*. H, holotype; SD, standard deviation. Values of Holotype included in range.

	H	range (n=15)	mean	SD
Standard length (mm)	110.6	78.1–153.4	–	–
Percentage of standard length				
Body depth	41.1	37.3–43.9	41.2	1.9
Predorsal length	43.7	42.6–47.8	45.1	1.6
Dorsal-fin base length	54.3	51.9–58.2	54.5	1.5
Last dorsal-fin spine length	15.2	12.9–16.0	14.4	0.9
Prepelvic length	45.6	41.8–47.0	45.0	1.5
Pelvic-fin length	30.9	25.6–34.1	29.1	2.4
Pelvic-fin spine length	13.4	11.7–14.4	13.0	0.8
Pectoral-fin length	31.4	28.0–33.6	29.2	8.5
Anal-fin base length	18.7	16.8–19.1	17.8	0.8
Last anal-fin spine length	13.3	12.5–15.1	13.1	0.7
Caudal peduncle length	17.3	12.3–17.5	15.4	2.0
Caudal peduncle depth	14.4	13.4–15.3	14.3	0.5
Head length	38.9	36.8–41.4	39.0	1.5
Percentage of head length				
Snout length	54	48–59	54.0	3.2
Preorbital depth	71	65–78	69.8	3.9
Head width	56	41–56	50.0	5.6
Head depth	89	84–95	88.5	3.6
Orbital diameter	23	18–27	23.7	2.8
Interorbital width	28	28–35	30.4	1.8
Upper jaw length	33	30–36	32.8	1.4
Lower jaw length	29	27–32	28.8	1.2

orangish hyaline. Pelvic-fin spine light orangish brown, anterior pelvic-fin rays light orangish brown with metallic greenish blue stripes parallel to rays, region around last rays hyaline.

Colouration in alcohol. Similar to colouration in life, except for metallic marks becoming dark brown on flank and light grey on fins; red and dark brown pigmentation fainted.

Distribution. Known only from the Rio Mariana, an isolated small coastal river of Bahia state, northeast Brazil (Fig. 3).

Etymology. The name *santosi* is in honour of Alexandre Clistenes Alcântara Santos, ichthyologist and friend, who is dedicated to the study of aquatic ecosystems of northeast Brazil.

Discussion

This study demonstrated that short fragments of the mitochondrial genome, with a total of 1780 bp, were enough to produce phylogenetic trees strongly supporting mutually exclusive lineages designated as species, as well as recognizing species clades with high support values (Fig. 1). However, presently no morphological character is known to unambiguously diagnose those clades.

Among the three main clades of the '*G.' brasiliensis* species group, the two species endemic to the Rio Paraguaçu Basin, *G. diamantinensis* and *G. obscurus*, form a well-supported basal clade (clade A), restricted to semi-arid areas of northeastern Brazil (Figs. 1 and 3). Interestingly, the analyses support another clade endemic to northeastern Brazil, between about 11° and 15° S, comprising *G. itapicuruensis* + *G. santosi* + *G. multiocellus* (clade B) that is sister to a geographically disjunct clade comprising *G. brasiliensis* + *G. rufomarginatus* + *G. iporangensis* (clade C), occurring in a vast area between about 16° and 35° S. Although a biogeographic analysis is beyond the scope of this study, the occurrence of two distinct basal lineages in northeastern Brazil, highly suggests that the most recent common ancestor of the '*G.' brasiliensis* species group was geographically restricted to northeastern Brazil.

The analyses also indicated that the main clades of the '*G.' brasiliensis* species group cannot be associated with specific biomes or phytogeographical provinces, in contrast to that recently reported for fish groups inhabiting temporary pools (Costa et al. 2017). Although the two species of the clade A being endemic to a semi-arid Caatinga area, only *G. itapicuruensis* inhabits a typical Caatinga area among species of the clade B. The other species of the clade C, *G. santosi* and *G. multiocellus*, are found in a transitional area of the Atlantic Forest known as Agreste. On the other hand, species of the clade C are found in different biomes such as Atlantic Forest, Cerrado and Pampas. Palynological studies have demonstrated a succession of different vegetation formations along the Pleistocene/Holocene of northeastern Brazil (Oliveira et al. 1999). Since members of different lineages of the '*G.' brasiliensis* species group are presently found in habitats such as rain forests and semi-arid regions, we conclude that vegetation changes following different climatic periods may have not affected fishes inhabiting rivers.

Acknowledgments

We are grateful to A. Kartz, A. Galvão, A. Santos, F. Ottoni, F. Fasura, G. Silva, M. Barbosa, O. Simões, P. Fasura and P. Bragança for help during field work or preparation of the manuscript. Financial support was given by CNPq (Conselho Nacional de Desenvolvimento Científico e Tecnológico – Ministério de Ciência e Tecnologia). Permits to field collections were provided by ICMBio (Instituto Chico Mendes de Conservação da Biodiversidade).

References

Alfaro ME, Holder MT (2006) The posterior and the prior in Bayesian phylogenetics. Annual Review of Ecology, Evolution, and Systematics 37: 19–42. https://doi.org/10.1146/annurev.ecolsys.37.091305.110021

Arbour JH, López-Fernández H (2014) Ecological variation in South American geophagine cichlids arose during an early burst of adaptive morphological and functional evolution. Proceedings of the Royal Society B 280: 20130849. http://dx.doi.org/10.1098/rspb.2013.0849

Chenna R, Sugawara H, Koike T, Lopez R, Gibson TJ, Higgins DG, Thompson JD (2003) Multiple sequence alignment with the Clustal series of programs. Nucleic Acids Research 31: 3497–3500. https://doi.org/10.1093/nar/gkg500

Close B, Banister K, Baumans V, Bernoth EM, Bromage N, Bunyan J, Erhardt W, Flecknell P, Gregory N, Hackbarth H, Morton D, Warwick C (1996) Recommendations for euthanasia of experimental animals: Part 1. Laboratory Animals 30: 293–316. https://doi.org/10.1258/002367796780739871

Close B, Banister K, Baumans V, Bernoth EM, Bromage N, Bunyan J, Erhardt W, Flecknell P, Gregory N, Hackbarth H, Morton D, Warwick C (1997) Recommendations for euthanasia of experimental animals: Part 2. Laboratory Animals 3: 1–32. https://doi.org/10.1258/002367797780600297

Costa WJEM (2006) Descriptive morphology and phylogenetic relationships among species of the Neotropical annual killifish genera *Nematolebias* and *Simpsonichthys* (Cyprinodontiformes: Aplocheiloidei: Rivulidae). Neotropical Ichthyology 4: 1–26. http://dx.doi.org/10.1590/S1679-62252006000100001

Costa WJEM, Amorim PF (2014) Integrative taxonomy and conservation of seasonal killifishes, *Xenurolebias* (Teleostei: Rivulidae), and the Brazilian Atlantic Forest. Systematics and Biodiversity 12: 350–365. https://doi.org/10.1080/14772000.2014.918062

Costa WJEM, Amorim PF, Aranha GN (2014) Species limits and DNA barcodes in *Nematolebias*, a genus of seasonal killifishes threatened with extinction from the Atlantic Forest of south-eastern Brazil, with description of a new species (Teleostei: Rivulidae). Ichthyological Exploration of Freshwaters 24: 225–236.

Costa WJEM, Cheffe MM, Amorim PF (2017) Two new seasonal killifishes of the *Austrolebias adloffi* group from the Lagoa dos Patos Basin, southern Brazil (Cyprinodontiformes: Aplocheilidae). Vertebrate Zoology 67: 139–149.

Costa WJEM, Amorim PF, Mattos JLO (2017) Molecular phylogeny and timing of diversification in South American Cynolebiini seasonal killifishes. Molecular Phylogenetics and Evolution 116: 61–68. https://doi.org/10.1016/j.ympev.2017.07.020

Darriba D, Taboada GL, Doallo R, Posada D (2012) jModelTest2: More models, new heuristics and parallel computing. Nature Methods 9: 772. https://doi.org/10.1038/nmeth.2109

Davis JI, Nixon KC (1992) Populations, genetic variation, and the delimitation of phylogenetic species. Systematic Biology 41: 421–435. https://doi.org/10.1093/sysbio/41.4.421

Farias IP, Ortí G, Sampaio L, Schneider H, Meyer A (2001) The cytochrome b gene as a phylogenetic marker: the limits of resolution for analyzing relationships among cichlid fishes. Journal of Molecular Evolution 53: 89–103. https://doi.org/10.1007/s002390010197

Felsenstein J (1985) Confidence limits on phylogenies: An approach using the bootstrap. Evolution 39: 783–791. https://doi.org/10.1111/j.1558-5646.1985.tb00420.x

Hillis DM, Bull JJ (1993) An empirical test of bootstrapping as a method for assessing confidence in phylogenetic analysis. Systematic Biology 42: 182–192. https://doi.org/10.1093/sysbio/42.2.182

Ilves KL, Torti D, López-Fernández H (2017) Exon-based phylogenomics strengthens the phylogeny of Neotropical cichlids and identifies remaining conflicting clades (Cichliformes: Cichlidae: Cichlinae). Molecular Phylogenetics and Evolution 118: 232–243. https://doi.org/10.1016/j.ympev.2017.10.008

Mabuchi K, Miya M, Azuma Y, Nishida M (2007) Independent evolution of the specialized pharyngeal jaw apparatus in cichlid and labrid fishes. BMC Evolutionary 7: 10. https://doi.org/10.1186/1471-2148-7-10

Kullander SO (1986) Cichlid fishes of the Amazon river drainage of Peru. Swedish Museum of Natural History, Stockholm, 431 pp.

Kullander SO (1998) A phylogeny and classification of the south american Cichlidae (Teleostei: Perciformes). In: Malabarba LR, Reis RE, Vari RP, Lucena ZM, Lucena CAS (Eds) Phylogeny and classification of Neotropical fishes, EDIPUCRS, Porto Alegre, 461–498.

Kullander SO (2003) Family Cichlidae (Cichlids). In: Reis RE, et al. (Eds) Check list of the freshwater fishes of South and Central America. EDIPUCRS, Porto Alegre, 605–654.

Lucena CAS, Kullander SO (2006) A review of the species of *Crenicichla* (Teleostei: Cichlidae) from the Atlantic coastal rivers of southeastern Brazil from Bahia to Rio Grande do Sul States, with descriptions of three new species. Neotropical Ichthyology 4: 127–146. https://doi.org/10.1590/S1679-62252006000200001

Kullander SO, Nijssen H (1989) The cichlids of Surinam (Teleostei: Labroidei). Brill, Leiden, 256 pp.

Leary S, Underwood W, Anthony R, Cartner S, Corey D, Grandin T (2013) AVMA Guidelines for the Euthanasia of Animals (2013 edn). http://works.bepress.com/cheryl_greenacre/14.

López-Fernández H, Arbour JH, Winemiller KO, Honeycutt RL (2013) Testing for ancient adaptive radiation in Neotropical cichlid fishes. Evolution 67: 1321–1337. https://doi.org/10.1111/evo.12038

López-Fernández H, Taphorn DC (2004) *Geophagus abalios*, *G. dicrozoster* and *G. winemilleri* (Perciformes: Cichlidae), three new species from Venezuela. Zootaxa 439: 1–27. https://doi.org/10.11646/zootaxa.439.1.1

López-Fernández HK, Winemiller O, Honeycut RL (2010) Multilocus phylogeny and rapid radiations in neotropical cichlid fishes (Perciformes: Cichlidae: Cichlinae). Molecular Phylogenetics and Evolution 55: 1070–1086. https://doi.org/10.1016/j.ympev.2010.02.020

Mattos JLO, Costa WJEM, Santos ACA (2015) *Geophagus diamantinensis*, a new species of the *G. brasiliensis* species group from Chapada Diamantina, north-eastern Brazil (Cichlid: Geophagini). Ichthyological Exploration of Freshwaters 26: 209–220.

Morrone JJ (2006) Biogeographic areas and transition zones of Latin America and the Caribbean islands based on panbiogeographic and cladistic analyses of the entomofauna. Annual Review of Entomology 51: 467–494. https://doi.org/10.1146/annurev.ento.50.071803.130447

Myers N, Mittermeier RA, Mittermeier CG, Fonseca GAB, Kent J (2000) Biodiversity hotspots for conservation priorities. Nature 403: 853–858. https://doi.org/10.1038/35002501

Nei M, Kumar S (2000) Molecular Evolution and Phylogenetics. Oxford University Press, New York, 333 pp.

Oliveira PE, Barreto AMF, Suguio K (1999) Late Pleistocene/Holocene climatic and vegetational history of the Brazilian caatinga: the fossil dunes of the middle São Francisco River. Palaeogeography, Palaeoclimatology, Palaeoecology 152: 319–337. https://doi.org/10.1016/S0031-0182(99)00061-9

Ottoni FP (2013) *Australoheros sanguineus* sp. n. – a new cichlid species from the rio Cubatão basin, southern Brazil (Cichlidae: Heroini). Vertebrate Zoology 63: 161–169.

Ottoni FP, Costa WJEM (2008) Taxonomic revision of the genus *Australoheros* Rican & Kullander, 2006 (Teleostei: Cichlidae) with descriptions of nine new species from southeastern Brazil. Vertebrate Zoology 58: 207–232.

Ronquist F, Teslenko M, van der Mark P, Ayres DL, Darling A, Höhna S, Larget B, Liu L, Suchard MA, Huelsenbeck JP (2012) MrBayes 3.2: Efficient Bayesian phylogenetic inference and model choice across a large model space. Systematic Biology 61: 539–542. https://doi.org/10.1093/sysbio/sys029

Rambaut A, Suchard MA, Xie D, Drummond AJ (2014) Tracer v1.6. http://tree.bio.ed.ac.uk/software/tracer/.

Smith WL, Chakrabarty P, Sparks JS (2008) Phylogeny, taxonomy, and evolution of Neotropical cichlids (Teleostei: Cichlidae: Cichlinae). Cladistics 24: 625–641. https://doi.org/10.1111/j.1096-0031.2008.00210.x

Swofford DL (2003) PAUP* Phylogenetic analysis using parsimony (*and other methods). Version 4. Sinauer Associates, Sunderland, Massachusetts.

Tamura K, Stecher G, Peterson D, Filipski A, Kumar S (2013) MEGA6: Molecular evolutionary genetics analysis version 6.0. Molecular Biology and Evolution 30: 2725–2729. https://doi.org/10.1093/molbev/mst197

Taylor WR, Van Dyke GC (1985) Revised procedures for staining and clearing small fishes and other vertebrates for bone and cartilage study. Cybium 9: 107–109. http://sfi.mnhn.fr/cybium/numeros/1985/92/01-Taylor%5b92%5d107-119.pdf

Wiens JJ, Penkrot TA (2002) Delimiting species using DNA and morphological variation and discordant species limits in spiny lizards (*Sceloporus*). Systematic Biolology 51: 69–91. https://doi.org/10.1080/106351502753475880

Zwickl DJ (2006) Genetic algorithm approaches for the phylogenetic analysis of large biological sequence datasets under the maximum likelihood criterion. Unpublished thesis, The University of Texas at Austin, 115 pp.